

Received:  
23 January 2018

Revised:  
15 August 2018

Accepted:  
15 September 2018

<https://doi.org/10.1259/bjr.20180101>

Cite this article as:

Yi A, Chang JM, Shin SU, Chu AJ, Cho N, Noh D-Y, et al. Detection of noncalcified breast cancer in patients with extremely dense breasts using digital breast tomosynthesis compared with full-field digital mammography. *Br J Radiol* 2019; **92**: 20180101.

## FULL PAPER

# Detection of noncalcified breast cancer in patients with extremely dense breasts using digital breast tomosynthesis compared with full-field digital mammography

<sup>1,2</sup>ANN YI, MD, <sup>1</sup>JUNG MIN CHANG, MD, <sup>1,2</sup>SUNG UI SHIN, MD, <sup>1</sup>A JUNG CHU, MD, <sup>1</sup>NARIYA CHO, MD, <sup>3</sup>DONG-YOUNG NOH, MD and <sup>1</sup>WOO KYUNG MOON, MD

<sup>1</sup>Department of Radiology, Seoul National University Hospital, Seoul, Republic of Korea

<sup>2</sup>Department of Radiology, Seoul National University Hospital Healthcare System Gangnam Center, Seoul, Republic of Korea

<sup>3</sup>Department of Surgery, Seoul National University Hospital, Seoul, Republic of Korea

Address correspondence to: Prof Jung Min Chang  
E-mail: [imchangjm@gmail.com](mailto:imchangjm@gmail.com)

**Objective:** To evaluate the tumour visibility and diagnostic performance of digital breast tomosynthesis (DBT) in patients with noncalcified  $T_1$  breast cancer.

**Methods:** Medical records of 106 females with noncalcified  $T_1$  invasive breast cancer who underwent DBT and full-field digital mammography (FFDM) between January 2012 and December 2014 were retrospectively reviewed. To assess tumour visibility (score 1-3), all DBT and FFDM images were reviewed by two radiologists blinded to clinicopathological information. A reference standard was established by an unblinded consensus review of all images. Clinicopathological and imaging variables were analysed based on tumour visibility. After adding 159 negative controls, the diagnostic performance of DBT + FFDM was compared with that of FFDM.

**Results:** The tumour visibility was significantly higher through DBT + FFDM (2.5 vs 1.8;  $p = 0.002$ ) than FFDM

alone. Breast composition was the independent variable for tumour visibility through DBT + FFDM (extremely dense; odds ratio, 0.02;  $p < 0.001$ ). Sensitivity ( $p = 0.642$ ), specificity ( $p = 0.463$ ), positive-predictive value ( $p = 0.078$ ), and negative-predictive value ( $p = 0.072$ ) of DBT + FFDM were not significantly superior to those of FFDM in 55 females with extremely dense breast composition, whereas specificity ( $p = 0.002$ ) and positive-predictive value ( $p < 0.001$ ) were significantly higher in 210 females with other breast compositions.

**Conclusion:** Addition of DBT to FFDM showed no significant increase in the tumour visibility and diagnostic performance in patients with noncalcified  $T_1$  cancer in extremely dense breasts.

**Advances in knowledge:** Addition of DBT to FFDM did not further improve the detection of noncalcified early breast cancers in females with extremely dense breasts.

## INTRODUCTION

Breast density-tailored screening for breast cancer in females is of great interest.<sup>1</sup> Breast density is a predictor of breast cancer; it reduces the sensitivity of mammography, leading to an increased risk of interval cancer in the screening population.<sup>2,3</sup> Several breast imaging modalities have been used as adjuncts to screening mammography in females with dense breasts, including ultrasound (US; handheld or automated), MRI, and the more recently applied digital breast tomosynthesis (DBT). DBT is an emerging technique that allows the breast to be viewed quasi-three-dimensionally, which reduces superimposition of the breast tissue.<sup>4,5</sup> Previous studies showed that DBT improved the accuracy of full-field digital mammography (FFDM) in screening across all breast densities by reducing

the recall rates and increasing the cancer detection rates.<sup>6-10</sup> In addition, a recent study including females with dense breasts reported that the addition of DBT increased the sensitivity of FFDM.<sup>11-13</sup>

To date, the effect of breast density on the diagnostic performance of DBT was evaluated based on percentage-based classification. Breast density assessed using mammography, reflects the breast composition. High breast density can comprise various breast compositions. The tumour located in the dense breast with small amount of interposed fat tissue that overlaps individual sections may result in mammographically occult cancer and even with the use of DBT.<sup>14</sup> Moreover, in case of the occurrence of small tumour without noticeable calcification,

the dense breast tissue might more easily obscure the tumour visibility.

We hypothesized that the visibility of small noncalcified breast cancers on DBT is affected by the breast composition. Therefore, the purpose of our study was to evaluate the tumour visibility and diagnostic performance of DBT in patients with noncalcified  $T_1$  breast cancers according to the breast composition.

## METHODS AND MATERIALS

### Study population

Our Institutional Review Board approved the retrospective study and waived the requirement for patients' informed consent. Of 2673 females who had undergone DBT and FFDM between January 2012 and December 2014, 106 females (median age, 51.2 years; age range, 22–77 years) who had undergone subsequent curative surgery for single noncalcified  $T_1$ -stage invasive breast cancer (median size, 8 mm; size range, 4–20 mm on surgical histopathology) were included. Among these patients, 68 females were referred from other hospitals with nonspecific clinical manifestation (64.2%), 31 females had a palpable lump (29.2%), and seven had nipple discharge (6.6%). The tumours were detected using DBT + FFDM ( $n = 91$ ), ultrasound ( $n = 103$ ), or both ( $n = 88$ ) at the time of diagnosis.

### Imaging data acquisition

All imaging data were acquired as part of our hospitals' routine clinical practice using an FFDM unit with integrated DBT acquisition (Selenia Dimensions mammography system, Hologic, Inc., Bedford, MA). Patients underwent bilateral two-view FFDM and DBT [craniocaudal (CC) and mediolateral oblique (MLO)] in the Combo mode, and FFDM and DBT images were obtained with single breast compression for each projection. In patients with the breast of 5.0 cm compressed thickness and 50 glandular fraction, DBT acquisition resulted in 8% higher mean glandular dose per view than that of digital mammography acquisition (1.30 and 1.20 mGy, respectively).

### Imaging data analysis

Four board-certified radiologists participated in the two retrospective review sessions. Each radiologist had more than 12 years' clinical experience in FFDM and more than 4 years' experience in DBT at the respective academic institution.

Table 1. Tumour visibility score: DBT + FFDM vs FFDM

Tumour visibility score	DBT + FFDM	FFDM	P-value <sup>a</sup>
1	22 (20.8)	56 (52.8)	0.011
2	11 (10.3)	13 (12.3)	
3	73 (68.9)	37 (34.9)	
Mean $\pm$ SD	2.5 $\pm$ 0.1	1.8 $\pm$ 0.2	0.002

DBT, digital breast tomosynthesis; FFDM, full-field digital mammography; SD, standard deviation.

Data are numbers of cases, and data in parentheses are percentages.

<sup>a</sup>P-values were obtained by the Pearson's Chi-square test for categorical variables and Mann-Whitney test for continuous variables.

### Tumour visibility

Two radiologists (JMC and AY) performed unblinded consensus review of the 106 tumour cases. First, the tumour site was determined on both the FFDM and DBT images and correlated with clinical, surgical, and pathologic findings. In case of uncertain tumour on the FFDM or DBT image, the estimated tumour locations were determined on the basis of the other imaging (ultrasound and MRI) findings. Subsequently, the visibility score (1–3) for the determined tumour location was assessed on both the DBT and FFDM images. The tumour that was obvious and conspicuous in both the CC and MLO views was assigned a score of 3; the tumour that was conspicuous in only one view or faintly visible was assigned a score of 2; and the tumour that was uncertain and not visible in both views was assigned a score of 1. The breast composition (a,b,c,d), and imaging characteristics of the mass (shape, margin, density) were determined per the Breast Imaging Reporting and Database System, fifth Edition.<sup>14</sup> In addition, the breast thickness (mm) at the time of mammographic image acquisition was recorded.

### Diagnostic performance

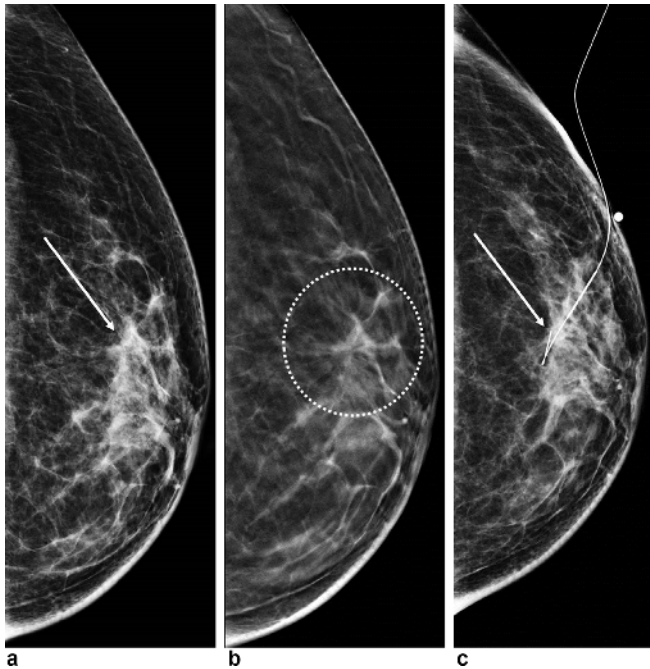
To assess the diagnostic performance, the other two radiologists (SUS and AJC) performed blinded consensus review of total 265 cases including 106 tumour cases, and 159 negative control cases. In addition, 159 negative control cases were identified from among the screening mammographies conducted between January 2012 and December 2014 with the results of final assessment Category 1, and absence of tumour occurrence after clinical or imaging follow-up for 1 year in our hospitals' medical report. The number of tumour cases and negative control cases were matched with a statistical ratio of 1:1.5 per breast composition.

Two separate review sessions were performed on the FFDM alone and DBT + FFDM images, respectively at 4 weeks' interval. In each reading session, all cases were randomized and presented in alternating order in a blinded manner with respect to the clinical, surgical, pathologic, and other imaging findings. With regard to the presence of suspected tumour on mammographic images, the presumptive tumour site was marked; and in case of the absence of suspected tumour, the images were left unmarked. Subsequently, the results of the blinded review were correlated with the reference data by two radiologists (JMC and AY) as follows: The case of tumour correctly marked on either CC and MLO views was assigned as true positive; the case of tumour wrongly marked or negative control case with marking was assigned as false positive; the negative control case with no marks was assigned as true negative; and the tumour case with no marks in any view was assigned as false-negative.

### Histopathological analysis

All 106 patients with tumours underwent curative surgery, including breast conserving surgery ( $n = 78$ ) and mastectomy ( $n = 28$ ). The tumour histology, histologic grade, and size (greatest dimension of the invasive tumour) were determined based on results obtained from the surgically excised specimens.<sup>15,16</sup> In addition, expression of the estrogen receptor (ER), progesterone receptor (PR), and human epidermal growth factor receptor Type 2 (HER2) was evaluated.<sup>17,18</sup> A cut-off value of 1% was used

Figure 1. Images of a 53-year-old female diagnosed with an invasive ductal carcinoma (0.9 cm in size) in the left breast (breast composition b). The left craniocaudal view on FFDM (a) showed an irregular hyperdense mass in the subareolar area of the left breast (visibility score 2). The left craniocaudal view on DBT (b) showed an irregular mass with more conspicuous spicules in the left breast (visibility score 3). Mammography-guided wire localization was performed (c). DBT, digital breast tomosynthesis; FFDM, full-field digital mammography.



to define ER and PR positivity.<sup>17</sup> HER2 expression was initially scored as 0, 1+, 2+, or 3+ based on results from the immunohistochemistry (IHC) staining; tumours with a score of 3+ were classified as HER2-positive, and tumours with a score of 0 or 1+ were classified as negative. In case of the tumour with score of 2+, gene amplification using fluorescence *in-situ* hybridization was used to determine the HER2 status. HER2 expression was considered as positive if the ratio of HER2 gene copies to chromosome 17 signals was >2.2. Moreover, the IHC subtypes were classified as ER positive (ER positive; and HER2 and PR positive or negative), HER2 enriched (HER2 positive; and ER and PR positive or negative), or triple negative (all ER, PR, and HER2 negative) subtypes.<sup>19</sup> A cutoff value of 14% was used to define Ki-67 positivity.<sup>20</sup>

### Statistical analysis

Tumour visibility scores were compared between the DBT + FFDM and FFDM images. The tumour visibility score on the DBT + FFDM images was correlated with the clinicopathological and imaging variables using Pearson's chi-square test or Fisher's exact test for categorical variables, and the Mann-Whitney test for continuous variables. Multivariate logistic regression analysis was performed to identify independent variables for the tumour visibility on the DBT + FFDM images. After stratification by independent variables, the diagnostic performance of DBT + FFDM was compared with that of FFDM according to the pathologic results or 12 months' clinical follow-up as reference standard.<sup>21,22</sup>

All statistical analyses were performed using Statistical Package for the Social Sciences for Windows, v. 19.0 (IBM Corp., Armonk, NY), and MedCalc for Windows, v. ersion 9.3.1, (MedCalc

Figure 2. Images of a 40-year-old female diagnosed with invasive ductal carcinoma (0.9 cm in size) combined with a ductal carcinoma *in situ* (2.1 cm in size) in the right breast (breast composition d). The right mediolateral oblique views of FFDM (a) and DBT (b) showed a uncertainly visible tumour (visibility score 1). A breast ultrasound (c) showed a discrete mass (1.3 cm in size) in the far upper outer area of the right breast. An isodense mass was demarcated on FFDM (d) after ultrasound-guided wire localization. DBT, digital breast tomosynthesis; FFDM, full-field digital mammography.

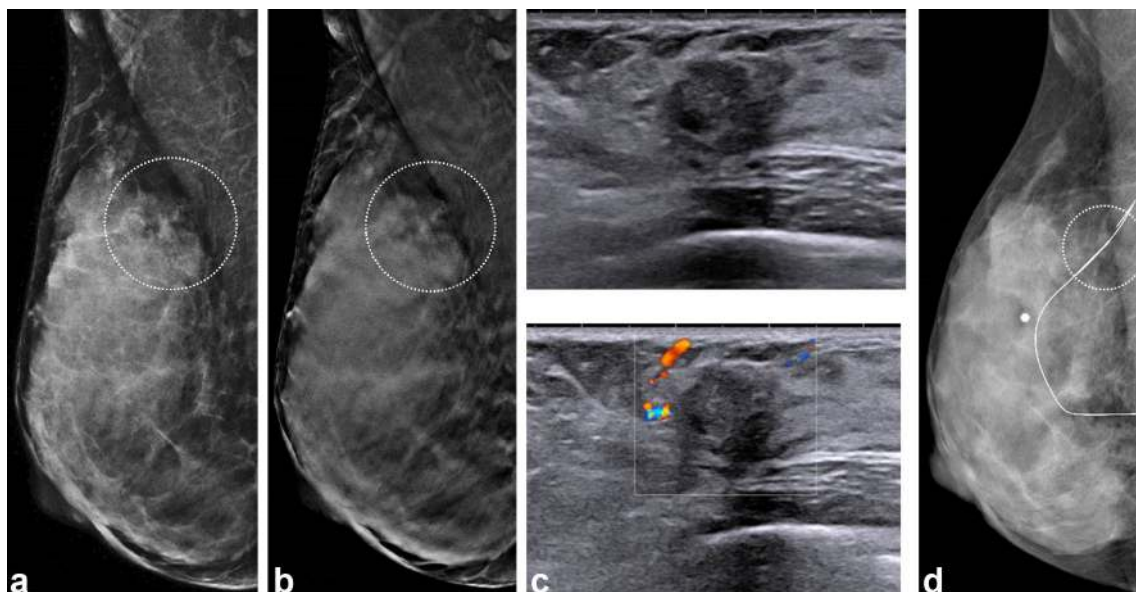


Table 2. Tumour visibility on DBT + FFDM and Clinicopathologic variables: Univariate analysis

Clinicopathologic variables	Total (n = 106)	Tumour visibility on DBT + FFDM			
		1 (n = 22)	2 (n = 11)	3 (n = 73)	P-value <sup>a</sup>
Age (years)					
Mean ± SD	52.2 ± 11.4 (range 22–77)	47.6 ± 7.9	50.6 ± 8.2	53.9 ± 12.3	0.078
Tumour size(mm) <sup>b</sup>					
Mean ± SD	14.6 ± 4.6 (range 4–20)	12.7 ± 5.1	12.7 ± 3.4	14.1 ± 4.6	0.728
Tumour histology					
Ductal	97 (91.5)	18 (81.8)	11 (100.0)	68 (93.2)	0.396
Lobular	5 (4.7)	2 (9.1)	0 (0)	3 (4.1)	
Others <sup>c</sup>	4 (3.8)	2 (9.1)	0 (0)	2 (2.7)	
Histologic grade					
1 or 2	55 (51.9)	13 (59.1)	7 (63.6)	35 (47.9)	0.468
3	51 (48.1)	9 (40.9)	4 (36.4)	38 (52.1)	
KI-67 (%)					
≤14	95 (89.6)	20 (90.9)	11 (100)	64 (87.7)	0.222
>14	11 (10.4)	2 (9.1)	0 (0)	9 (12.3)	
IHC subtype					
ER-positive	86 (81.1)	20 (90.9)	9 (81.8)	57 (78.1)	0.318
HER2-enriched	10 (9.4)	2 (9.1)	0 (0)	8 (11.0)	
Triple negative	10 (9.4)	0 (0)	2 (18.2)	8 (11.0)	

DBT, digital breast tomosynthesis; FFDM, full-field digital mammography; SD, standard deviation; ER, estrogen receptor; HER2, human epidermal growth factor receptor 2; IHC, immuno histo chemistry.

Data are numbers of cases, and data in parentheses are percentages.

<sup>a</sup>P-values were obtained by the Pearson's Chi-square test or Fisher's exact test for categorical variables and Mann-Whitney test for continuous variables. P-value < 0.050 was considered to indicate a statistically significant difference.

<sup>b</sup>Determined by the greatest dimension of the invasive tumour on the basis of the surgically excised specimens.

<sup>c</sup>Papillary (n = 2, 1.9%), mucinous (n = 1, 0.9%), and tubular (n = 1, 0.9%) cancers.

Software, Mariakerke, Belgium). P-value of less than 0.05 was considered as significant.

## RESULTS

### Tumour visibility

The surgical histopathology revealed that of 106 tumours, 97 (91.5%) were ductal, 5 (4.7%) were lobular, 2 (1.9%) were papillary, 1 (0.9%) was mucinous, and 1 (0.9%) was tubular carcinoma. Molecular subtypes included the ER positive (n = 86, 81.1%), HER2 enriched (n = 10, 9.4%), and triple negative (n = 10, 9.4%) subtypes.

Tumour visibility scores are listed in Table 1. The tumour visibility score was significantly higher in the DBT + FFDM images (mean, 2.5 vs 1.8; p = 0.002) than that in the FFDM images (Figures 1 and 2). Univariate analysis revealed that the breast composition (p < 0.001) and mass density (p = 0.006) were associated with the tumour visibility through DBT + FFDM (Tables 2 and 3). Multivariate logistic regression analysis revealed that composition d (odds ratio, 0.02; p < 0.001) was independently associated with poor tumour visibility through DBT + FFDM (Table 4).

### Diagnostic performance

The diagnostic performance of FFDM vs DBT + FFDM in 265 cases is described in Table 5. The diagnostic performance of DBT + FFDM including sensitivity (63.6% vs 59.1%; p = 0.642), specificity (84.8% vs 75.8%; p = 0.463), positive-predictive value (79.2% vs 61.9%; p = 0.078), and negative-predictive value (90.3% vs 73.5%; p = 0.072) was not significantly superior to those of FFDM in 55 females with composition d breast, whereas specificity (98.4% vs 81.7%; p = 0.002) and positive-predictive value (97.6% vs 76.8%; p < 0.001) were significantly higher in 210 females with the other breast compositions.

## DISCUSSION

The results of our study indicated that the addition of DBT did not significantly increase the tumour visibility and diagnostic performance of FFDM for noncalcified T<sub>1</sub> cancers in patients with breast composition d. Recent studies demonstrated that the use of DBT + FFDM is likely to show a decrease in the rate of false-positive results, and an increase in the cancer-detection rate compared with the use of FFDM alone, despite presence of the dense breasts.<sup>6–13</sup> In these studies, the breast density was assessed as an approximate percentage value of

Table 3. Tumour visibility on DBT + FFDM and Imaging variables: Univariate analysis

Imaging variables	Total (n = 106)	Tumour visibility on DBT + FFDM			
		1 (n = 22)	2 (n = 11)	3 (n = 73)	P-value <sup>a</sup>
Breast composition					
a	22 (20.8)	0 (0)	1 (9.1)	21 (28.8)	<0.001
b	18 (17.0)	0 (0)	1 (9.1)	17 (23.3)	
c	44 (41.5)	5 (22.7)	9 (81.8)	30 (41.1)	
d	22 (20.8)	17 (77.3)	0 (0)	5 (6.8)	
Breast thickness (mm) <sup>b</sup>					
Mean ± SD	45.8 ± 11.0 (range 11.0–67.8)	41.2 ± 11.6	51.2 ± 9.2	46.4 ± 10.7	0.211
Mass shape					
Oval or round	24 (22.6)	2 (9.1)	3 (27.3)	19 (26.0)	0.232
Irregular	82 (77.4)	20 (90.9)	8 (72.7)	54 (74.0)	
Mass margin					
Circumscribed	5 (4.7)	0 (0)	2 (18.2)	3 (4.1)	0.061
Not-circumscribed	101 (95.3)	22 (100)	9 (81.9)	70 (95.9)	
Mass density					
Iso	37 (34.9)	14 (63.6)	3 (27.3)	20 (27.4)	0.006
Hyper	69 (65.1)	8 (36.4)	8 (72.7)	53 (72.6)	

DBT, digital breast tomosynthesis; FFDM, full-field digital mammography; SD, standard deviation.

Data are numbers of cases, and data in parentheses are percentages.

<sup>a</sup>P-values were obtained by the Pearson's Chi-square test or Fisher's exact test for categorical variables and Mann-Whitney test for continuous variables. P-value < 0.050 was considered to indicate a statistically significant difference.

<sup>b</sup>Automatically measured at the time of mammographic image acquisition.

the fibroglandular tissue in relation to the whole breast area on mammography scans. Rafferty et al reported that addition of DBT to FFDM for screening purpose was associated with improved diagnostic performance in both females with the dense and non-dense breast tissue; however, the combined gain was largest in those with composition *c*, but not significant in those with composition *d*.<sup>23</sup> In case of the lesion located in the extremely dense breast without interposed radiolucent fat densities that overlaps individual sections on the DBT image, a false-negative result may be obtained. Accordingly, our results showed that added DBT to FFDM was not equally effective in all females with the dense breast. In addition, in case of the lesion comprising noncalcified isodense small cancer obscured in dense fibroglandular tissue, there is high probability of failed detection on both the DBT and FFDM images. Therefore, requirement of interfacing between the radiodense

fibroglandular tissue and radiolucent fat tissue might be a necessary precondition for effective application of DBT in patients with the dense breast.<sup>24</sup>

The tumour visibility through DBT might be affected by the morphologic features of the tumour despite the low statistical significance of our results. Reports have indicated that breast cancers showed different imaging features according to their molecular subtype.<sup>25</sup> In our study, since we only included *T*<sub>1</sub> stage cancers, the total number of cancers was small; hence, there is limitation to generalizing our data. However, Lee et al reported that in patients undergoing DBT, despite the finding of characteristic imaging features of breast cancer per molecular subtype, cancer detectability on the DBT image was unaffected by molecular subtype of the breast cancer.<sup>26</sup>

Table 4. Tumour visibility on DBT + FFDM: Multivariate analysis

Variables	Multivariate analysis		
	Odds ratio	95% Confidence interval	P-value <sup>a</sup>
Breast composition: grade <i>d</i>	0.02	0.04–0.09	<0.001
Mass density: isodense	0.29	0.07–1.15	0.203

DBT, digital breast tomosynthesis; FFDM, full-field digital mammography.

<sup>a</sup>P-values were obtained by the multivariate logistic regression model after controlling for significant variables (p-value < 0.05 on univariate analysis in Table 2).

Table 5. Diagnostic performance according to breast composition: DBT + FFDM vs FFDM

		Composition a,b,c (n = 210) <sup>a</sup>			Composition d (n = 55) <sup>b</sup>		
		DBT + FFDM	FFDM	P-value	DBT + FFDM	FFDM	P-value
Diagnostic performance (%)	Sensitivity	95.2 (80/84)	90.5 (76/84)	0.451	63.6 (14/22)	59.1 (13/22)	0.642
	Specificity	98.4 (124/126)	81.7 (103/126)	0.002	84.8 (28/33)	75.8 (25/33)	0.463
	Positive predictive value	97.6 (80/82)	76.8 (76/99)	<.001	79.2 (19/24)	61.9 (13/21)	0.078
	Negative predictive value	96.9 (124/128)	92.8 (103/111)	0.589	90.3 (28/31)	73.5 (25/34)	0.072

DBT, digital breast tomosynthesis; FFDM, full-field digital mammography.

Note.—Data in parentheses are the raw figures from which the percentages were calculated.

<sup>a</sup>84 tumour cases and 126 negative controls.

<sup>b</sup>22 tumour cases and 33 negative controls.

<sup>c</sup>P-values were obtained by the McNemar test. P-value <0.050 was considered to indicate a statistically significant difference.

A study comparing DBT and ultrasound reported limited diagnostic values of DBT in patients with breasts with composition *d*.<sup>27</sup> Moreover, despite equivalent overall performances, the diagnostic performance of ultrasound tended to be high in participants with breast composition *d*, with higher sensitivity than that of DBT.<sup>13</sup> In our study, among the 22 tumours located in breasts with composition *d*, 8 (36.4%) tumours were not detected on both the DBT and FFDM images, but all tumours were visible through prospective ultrasound performed at the time of initial diagnosis. MRI or contrast-enhanced mammography were indicated as supplemental imaging modalities in females with dense breasts according to the individuals' risk level.<sup>28–30</sup> Therefore, studies aimed to optimize the imaging modalities, screening intervals, and assessment of patients' individual and familial risk are required to develop optimal strategy for breast cancer screening in females with breast composition *d*.

Our study had several limitations. First, this was a retrospective study including a relatively small sample size. Of the cohort of 106 females, only 22 females had breasts with composition *d*. Further investigation including a larger study population is necessary. Second, we performed consensus review sessions but did not assess the inter- or intraobserver variance; however, through discussion of results between the two radiologists, the best concordant results were determined. In addition, assessment of the tumour visibility was performed in an unblinded manner with regard to the tumour location. Although the unblinded review may have

bias, assessment of the tumour visibility is required to determine the exact tumour site on the mammographic images. Fourth, our study population was limited to noncalcified *T*<sub>1</sub> breast cancer in Asian females; future studies are required to reassess the diagnostic performance of DBT compared with FFDM for all stages of tumours across characteristic of all breast densities and races. Finally, this was a single-institution study focused on FFDM and DBT by a single manufacturer. Further study including a larger population is necessary to determine optimum imaging strategy in such patients.

In conclusion, breast composition was significantly associated with the tumour visibility and diagnostic performance of DBT + FFDM in the evaluation of females with noncalcified *T*<sub>1</sub> invasive breast cancer. Addition of DBT to FFDM showed no further improvement in the rate of diagnostic accuracy of noncalcified *T*<sub>1</sub> breast cancer in females with breast composition *d*. Therefore, for screening of females with breast composition *d*, the use of supplemental imaging other than DBT may be considered even though large prospective studies are warranted.

#### ACKNOWLEDGMENT

This research was supported by a grant of the Korea Health Technology R&D Project through the Korea Health Industry Development Institute (KHIDI), funded by the Ministry of Health & Welfare, Republic of Korea (grant number : HI15C1532). Kyung Sook Yang kindly provided statistical advice for this manuscript.

#### REFERENCES

- Melnikow J, Fenton JJ, Whitlock EP, Miglioretti DL, Weyrich MS, Thompson JH, et al. Supplemental screening for breast cancer in women with dense breasts: a systematic review for the U.S. Preventive Services Task Force. *Ann Intern Med* 2016; **164**: 268–78. doi: <https://doi.org/10.7326/M15-1789>
- McCormack VA, dos Santos Silva I, Silva DS I. Breast density and parenchymal patterns as markers of breast cancer risk: a meta-analysis. *Cancer Epidemiol Biomarkers Prev* 2006; **15**: 1159–69. doi: <https://doi.org/10.1158/1055-9965.EPI-06-0034>
- Kerlikowske K, Zhu W, Tosteson AN, Sprague BL, Tice JA, Lehman CD, et al. Identifying women with dense breasts at high risk for interval cancer: a cohort study. *Ann Intern Med* 2015; **162**: 673–81. doi: <https://doi.org/10.7326/M14-1465>
- Helvie MA. Digital mammography imaging: breast tomosynthesis and advanced applications. *Radiol Clin North Am* 2010; **48**: 917–29. doi: <https://doi.org/10.1016/j.rcl.2010.06.009>
- Houssami N, Skaane P. Overview of the evidence on digital breast tomosynthesis in breast cancer detection. *Breast* 2013; **22**: 101–8. doi: <https://doi.org/10.1016/j.breast.2013.01.017>
- McDonald ES, Oustimov A, Weinstein SP, Synnestvedt MB, Schnall M, Conant EF. Effectiveness of digital breast tomosynthesis

- compared with digital mammography: outcomes analysis from 3 years of breast cancer screening. *JAMA Oncol* 2016; **2**: 737–43. doi: <https://doi.org/10.1001/jamaoncol.2015.5536>
7. Ciatto S, Houssami N, Bernardi D, Caumo F, Pellegrini M, Brunelli S, et al. Integration of 3D digital mammography with tomosynthesis for population breast-cancer screening (STORM): a prospective comparison study. *Lancet Oncol* 2013 Jun; **14**: 583–9. doi: [https://doi.org/10.1016/S1470-2045\(13\)70134-7](https://doi.org/10.1016/S1470-2045(13)70134-7)
  8. Skaane P, Bandos AI, Gullien R, Eben EB, Ekseth U, Haakenaasen U, et al. Comparison of digital mammography alone and digital mammography plus tomosynthesis in a population-based screening program. *Radiology* 2013; **267**: 47–56. doi: <https://doi.org/10.1148/radiol.12121373>
  9. Skaane P, Bandos AI, Gullien R, Eben EB, Ekseth U, Haakenaasen U, et al. Prospective trial comparing full-field digital mammography (FFDM) versus combined FFDM and tomosynthesis in a population-based screening programme using independent double reading with arbitration. *Eur Radiol* 2013; **23**: 2061–71. doi: <https://doi.org/10.1007/s00330-013-2820-3>
  10. Friedewald SM, Rafferty EA, Rose SL, Durand MA, Plecha DM, Greenberg JS, et al. Breast cancer screening using tomosynthesis in combination with digital mammography. *JAMA* 2014; **311**: 2499–507. doi: <https://doi.org/10.1001/jama.2014.6095>
  11. Gilbert FJ, Tucker L, Gillan MG, Willsher P, Cooke J, Duncan KA, et al. Accuracy of digital breast tomosynthesis for depicting breast cancer subgroups in a UK retrospective reading study (TOMMY Trial). *Radiology* 2015; **277**: 697–706. doi: <https://doi.org/10.1148/radiol.2015142566>
  12. Houssami N, Turner RM. Rapid review: Estimates of incremental breast cancer detection from tomosynthesis (3D-mammography) screening in women with dense breasts. *Breast* 2016; **30**: 141–5. doi: <https://doi.org/10.1016/j.breast.2016.09.008>
  13. Tagliafico AS, Calabrese M, Mariscotti G, Durando M, Tosto S, Monetti F. Adjunct screening with tomosynthesis or ultrasound in women with mammography-negative dense breasts: interim report of a prospective comparative trial. *J Clin Oncol* 2016; **9**: JCO634147.
  14. Sickles EA, D'Orsi CJ, Bassett LW, Appleton CM, Berg WA, Burnside ES. ACR BI-RADS Mammography. In: Reston, ed. *ACR BI-RADS Atlas, Breast Imaging Reporting and Data System*. 5th; 2013.
  15. Elston CW, Ellis IO. Pathological prognostic factors in breast cancer. I. The value of histological grade in breast cancer: experience from a large study with long-term follow-up. *Histopathology* 2002; **41**(3A): 154–61.
  16. Edge SB, Compton CC. The American Joint Committee on Cancer: the 7th edition of the AJCC cancer staging manual and the future of TNM. *Ann Surg Oncol* 2010; **17**: 1471–4.
  17. Hammond ME, Hayes DF, Dowsett M, Allred DC, Hagerty KL, Badve S, et al. American Society of Clinical Oncology/ College Of American Pathologists guideline recommendations for immunohistochemical testing of estrogen and progesterone receptors in breast cancer. *J Clin Oncol* 2010; **28**: 2784–95. doi: <https://doi.org/10.1200/JCO.2009.25.6529>
  18. Wolff AC, Hammond ME, Schwartz JN, Hagerty KL, Allred DC, Cote RJ, et al. American Society of Clinical Oncology/ College of American Pathologists guideline recommendations for human epidermal growth factor receptor 2 testing in breast cancer. *J Clin Oncol* 2007; **25**: 118–45. doi: <https://doi.org/10.1200/JCO.2006.09.2775>
  19. Goldhirsch A, Wood WC, Coates AS, Gelber RD, Thürlimann B, Senn HJ, et al. Strategies for subtypes--dealing with the diversity of breast cancer: highlights of the St. Gallen International Expert Consensus on the Primary Therapy of Early Breast Cancer 2011. *Ann Oncol* 2011; **22**: 1736–47. doi: <https://doi.org/10.1093/annonc/mdr304>
  20. Cheang MC, Chia SK, Voduc D, Gao D, Leung S, Snider J, et al. Ki67 index, HER2 status, and prognosis of patients with luminal B breast cancer. *J Natl Cancer Inst* 2009; **101**: 736–50. doi: <https://doi.org/10.1093/jnci/djp082>
  21. McNEMAR Q. Note on the sampling error of the difference between correlated proportions or percentages. *Psychometrika* 1947; **12**: 153–7. doi: <https://doi.org/10.1007/BF02295996>
  22. Breslow NE, Day NE. *Statistical methods in cancer research: vol 1—the analysis of case-control studies*. Lyon, France: IARC; 1981.
  23. Rafferty EA, Durand MA, Conant EF, Copit DS, Friedewald SM, Plecha DM, et al. Breast cancer screening using tomosynthesis and digital mammography in dense and nondense breasts. *JAMA* 2016; **315**: 1784–6. doi: <https://doi.org/10.1001/jama.2016.1708>
  24. Peppard HR, Nicholson BE, Rochman CM, Merchant JK, Mayo RC, Harvey JA. Digital breast tomosynthesis in the diagnostic setting: indications and clinical applications. *Radiographics* 2015; **35**: 975–90. doi: <https://doi.org/10.1148/rg.2015140204>
  25. Tamaki K, Ishida T, Miyashita M, Amari M, Ohuchi N, Tamaki N, et al. Correlation between mammographic findings and corresponding histopathology: potential predictors for biological characteristics of breast diseases. *Cancer Sci* 2011; **102**: 2179–85. doi: <https://doi.org/10.1111/j.1349-7006.2011.02088.x>
  26. Lee SH, Chang JM, Shin SU, Chu AJ, Yi A, Cho N, et al. Imaging features of breast cancers on digital breast tomosynthesis according to molecular subtype: association with breast cancer detection. *Br J Radiol* 2017; **90**: 20170470. doi: <https://doi.org/10.1259/bjr.20170470>
  27. Kim WH, Chang JM, Lee J, Chu AJ, Seo M, Gweon HM, et al. Diagnostic performance of tomosynthesis and breast ultrasonography in women with dense breasts: a prospective comparison study. *Breast Cancer Res Treat* 2017; **162**: 85–94. doi: <https://doi.org/10.1007/s10549-017-4105-z>
  28. Berg WA, Zhang Z, Lehrer D, Jong RA, Pisano ED, Barr RG, et al. Detection of breast cancer with addition of annual screening ultrasound or a single screening MRI to mammography in women with elevated breast cancer risk. *JAMA* 2012; **307**: 1394–404. doi: <https://doi.org/10.1001/jama.2012.388>
  29. Lewin J. Comparison of contrast-enhanced mammography and contrast-enhanced breast MR imaging. *Magn Reson Imaging Clin N Am* 2018; **26**: 259–63. doi: <https://doi.org/10.1016/j.mric.2017.12.005>
  30. Emaus MJ, Bakker MF, Peeters PH, Loo CE, Mann RM, de Jong MD, et al. MR imaging as an additional screening modality for the detection of breast cancer in women aged 50–75 years with extremely dense breasts: the DENSE trial study design. *Radiology* 2015; **277**: 527–37. doi: <https://doi.org/10.1148/radiol.2015141827>